

MULTI-OBJECTIVE OPTIMIZATION OF THE INNER REINFORCEMENT FOR A VEHICLE'S HOOD CONSIDERING STATIC STIFFNESS AND NATURAL FREQUENCY

S. H. CHOI¹⁾, S. R. KIM¹⁾, J. Y. PARK¹⁾ and S. Y. HAN^{2)*}

¹⁾Department of Mechanical Engineering, Graduate School, Hanyang University, Seoul 133-791, Korea

²⁾School of Mechanical Engineering, Hanyang University, Seoul 133-791, Korea

(Received 12 March 2007; Revised 15 May 2007)

ABSTRACT—A multi-objective optimization technique was implemented to obtain optimal topologies of the inner reinforcement for a vehicle's hood simultaneously considering the static stiffness of bending and torsion and natural frequency. In addition, a smoothing scheme was used to suppress the checkerboard patterns in the ESO method. Two models with different curvature were chosen in order to investigate the effect of curvature on the static stiffness and natural frequency of the inner reinforcement. A scale factor was employed to properly reflect the effect of each objective function. From several combinations of weighting factors, a Pareto-optimal topology solution was obtained. As the weighting factor for the elastic strain efficiency went from 1 to 0, the optimal topologies transmitted from the optimal topology of a static stiffness problem to that of a natural frequency problem. It was also found that the higher curvature model had a larger static stiffness and natural frequency than the lower curvature model. From the results, it is concluded that the ESO method with a smoothing scheme was effectively applied to topology optimization of the inner reinforcement of a vehicle's hood.

KEY WORDS : Multi-objective optimization, Static stiffness, Natural frequency, Smoothing scheme, Inner reinforcement of a vehicle's hood, Topology optimization

1. INTRODUCTION

Shell and plate structures such as a vehicle's hood and trunk, of which the areas are very wide compared to their thicknesses, are very weak in both transverse loading and transverse vibration. Therefore, they have been used with inner reinforcement attached beneath the structures. In order to design inner reinforcement of the structures, a topology optimization should be performed. The optimum topology of reinforcement is very important in weight reduction and fuel efficiency improvement of a vehicle.

In order to obtain an optimum design under the required design conditions, the concept of optimum design such as design sensitivity analysis should be implemented in addition to estimations for static stiffness and natural frequency (Lee *et al.*, 2000). Topology optimization techniques are used to obtain optimal topologies by determining which elements should remain inside the structure under the required constraints. An important recent development in this area was made by Bendsøe and Kikuchi (Bendsøe and Kikuchi, 1988) who proposed the

homogenization method, in which the structure is represented by a model with micro voids and the objective is to seek the optimal porosity of the porous medium. Recently, evolutionary structural optimization (ESO) has been proposed by Xie and Steven (1994; Chu *et al.*, 1996; Li *et al.*, 2000), based on the concept of gradually removing redundant elements to obtain an optimal topology.

In this study, optimal topology of the inner reinforcement for a vehicle's hood simultaneously considering the static stiffness of bending and torsion, and natural frequency was obtained by the ESO method. To accomplish this, the multi-objective design optimization technique was implemented and a scale factor was employed to properly reflect the effect of each objective function. A smoothing scheme (Li *et al.*, 2000) was applied to suppress the checkerboard patterns during the procedure of topology optimization. Also, two models with different curvature were chosen in order to investigate the effect of curvature on static stiffness and on the natural frequency of the inner reinforcement.

*Corresponding author. e-mail: syhan@hanyang.ac.kr

2. MULTI-OBJECTIVE DESIGN OPTIMIZATION

Multi-objective design optimization is a design method used to simultaneously maximize more than one objective function. In this case, weighting factors can be introduced to reflect the importance of different design criteria such as static stiffness and natural frequency. Using several combinations of weighting factors, different trade-off strategies result in different topologies. Each of these topologies represents a Pareto-optimal solution (Li *et al.*, 2000). Therefore, a designer can select an optimal solution from the Pareto-optimal solution dependent on the level of importance.

2.1. Multi-objective Sensitivity Number for Static Stiffness

The sensitivity number for static stiffness (Chu *et al.*, 1996) is generally defined by Equation (1). Equation (1) calculates the change in the elastic strain energy in a structure when the i^{th} element is removed. Therefore, an optimal topology of a structure having the maximum static stiffness is obtained by removing gradually the elements which have the lowest sensitivity numbers for static stiffness. The multi-objective sensitivity number for static stiffness can be obtained by Equation (2) by imposing the weighting factors on the sensitivity numbers for bending and torsion in order to reflect the importance of bending and torsion, respectively.

$$\alpha_{si}^e = \frac{1}{2} \{u^i\}^T [K^i] \{u^i\} \quad (i=1, n) \quad (1)$$

$$\alpha_{ss}^e = \left[\lambda_1^s \left(\frac{\alpha_b^e - \alpha_{b\min}}{\alpha_{b\max} - \alpha_{b\min}} \right) + \lambda_2^s \left(\frac{\alpha_t^e - \alpha_{t\min}}{\alpha_{t\max} - \alpha_{t\min}} \right) \right] \quad (2)$$

In these equations, α_{si}^e is the strain energy of each element, $\{u^i\}$ is the displacement vector of the i -th element, $[K^i]$ is the stiffness matrix of the i -th element, λ_1 and λ_2 are weighting factors for bending and torsion, respectively, α_b^e is the strain energy of each element due to bending, and α_t^e is the strain energy of each element due to torsion.

Since the obtained multi-objective sensitivity number for static stiffness should be combined with the sensitivity number for natural frequency, it is normalized by Equation (3),

$$\alpha_{Nss}^e = \frac{\alpha_{ss}^e - \alpha_{ss\min}}{\alpha_{ss\max} - \alpha_{ss\min}} \quad (3)$$

where, α_{ss}^e is the sensitivity number for static stiffness, and $\alpha_{ss\max}$ and $\alpha_{ss\min}$ are the maximum and minimum sensitivity numbers for static stiffness, respectively.

2.2. Sensitivity Number for Natural Frequency

The sensitivity number for natural frequency is defined by Equation (4). Equation (4) estimates the difference

between the kinetic energy and elastic strain energy in a structure when the i^{th} element is removed (Sigmund and Petersson, 1998). An increase or decrease in natural frequency can be accomplished by removing the elements having the highest or the lowest sensitivity numbers in the ESO. In general, the natural frequency of a structure is designed to be as large as possible because it is helpful to avoid resonance in a structure. Therefore, an optimal topology of a structure having the maximum natural frequency is obtained by gradually removing the elements which have the highest sensitivity numbers for natural frequency. In order to combine sensitivity numbers for natural frequency with those for static stiffness, the sensitivity numbers can be normalized by the following Equation (5),

$$\alpha_{di}^e = \frac{1}{m_i} \{u_i^e\}^T (\omega_i^2 [M^e] - [K^e]) \{u_i^e\} \quad (4)$$

$$\alpha_{Ndi}^e = 1 - \left(\frac{\alpha_{di}^e - \alpha_{d\min}}{\alpha_{d\max} - \alpha_{d\min}} \right) \quad (5)$$

where α_{di}^e is the sensitivity number for natural frequency, m_i is the mass of the i -th element, $\{u_i^e\}$ denotes the eigenvector corresponding to ω_i , ω_i is the i -th natural frequency, $[M^e]$ is the mass matrix, $[K^e]$ is the stiffness matrix, and $\alpha_{d\max}$ and $\alpha_{d\min}$ are the maximum and minimum sensitivity numbers for natural frequency, respectively.

2.3. Multi-objective Sensitivity Number for Static Stiffness and Natural Frequency

The multi-objective sensitivity number for both static stiffness and natural frequency is obtained by the following Equation (6) by imposing the weighting factors on sensitivity numbers for static stiffness and natural frequency in order to reflect the importance of static stiffness and natural frequency, respectively.

$$\alpha_{mi}^e = \lambda_1^m \left(\frac{\alpha_{Nss}^e}{sfs} \right) + \lambda_2^m \left(\frac{\alpha_{Ndi}^e}{sfd} \right) \quad (6)$$

In Equation 6, sfs and sfd are scale factors, which are employed to make the averages of the normalized sensitivity number for static stiffness, α_{Nss}^e , and the normalized sensitivity number of natural frequency, α_{Ndi}^e , equal. α_{mi}^e is the multi-objective sensitivity number of each element.

2.4. Removal Line

Optimal topology based on ESO is obtained by gradually removing the elements having the lowest multi-objective sensitivity numbers for static stiffness and natural frequency. In order to determine the elements to be removed, the removal line should be established. The normalized multi-objective sensitivity number for static stiffness and natural frequency lies between 0 and 1. Since the weight-

ing factors, λ_1^m and λ_2^m , and the scale factors, sfs and sfd , are imposed to the normalized multi-objective sensitivity number for static stiffness and natural frequency, the values become greater than 0 and smaller than 1. This creates difficulty in establishing the removal line, so Equation (6) must be normalized by Equation (7) once again,

$$\alpha_{Nmi}^f = \frac{\alpha_{mi}^f - \alpha_{mimin}}{\alpha_{mimax} - \alpha_{mimin}} \quad (7)$$

where α_{Nmi}^f is the normalized multi-objective sensitivity number for static stiffness and natural frequency and α_{dmax} and α_{dmin} are the maximum and minimum normalized multi-objective sensitivity numbers for natural frequency, respectively.

The removal line can be established as Equation (8) where the threshold rate, $\Delta\alpha$, is a value obtained empirically.

$$RL = \alpha_{Nmimin} \times \Delta\alpha \quad (8)$$

The elements for which the normalized multiobjective sensitivity number for static stiffness and natural frequency, α_{Nmi}^f , are less than or equal to RL are to be removed. This condition can be expressed by the following Equation (9).

$$\alpha_{Nmi}^f \leq RL \quad (9)$$

This process is iterated until the obtained topology satisfies the restricted conditions of mass, yield stress, and deflection.

3. SUPPRESSION OF CHECKERBOARD PATTERNS

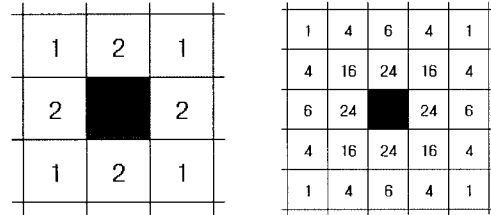
Checkerboard patterns are quite common in various finite element-based structural optimization techniques. As pointed out in previous research (Sigmund and Petersson, 1998), four-node element meshes appear to be locally stiffer than any real material. Shapes and topologies produced with checkerboard patterns may be unacceptable for practical applications. For this reason, the suppression of the checkerboard pattern has recently attracted considerable attention. To correct this, an intuitive smoothing technique (Li *et al.*, 2000) was introduced which consists of two basic steps:

- (1) Calculate the sensitivity number at each node by using a volumetric weighted average of the sensitivity number for each element connected to this node.
- (2) Calculate the new sensitivity number for an element by calculating the average of the nodal sensitivity numbers for that element.

The weighting factors for each element are shown in Figure 1, and were classified into the first and the second

order schemes due to the number of layers surrounding the center element. This is viewed as a first order smoothing technique. For a regular rectangular mesh, the efficiency of the smoothed element is calculated from itself and those of 8 surrounding elements in the first surrounding layer shown in Figure 1(a). When necessary, a second order smoothing approach may be applied, in which the smoothed efficiency factors are further smoothed. For a rectangular mesh, the efficiency of the smoothed element is calculated from itself and those of 24 surrounding elements in the first and second layers shown in Figure 1(b).

A new sensitivity number for the center element when applying the smoothing technique can be expressed by



(a) First order scheme (b) Second order scheme

Figure 1. Filter parameter for the checkerboard suppression.

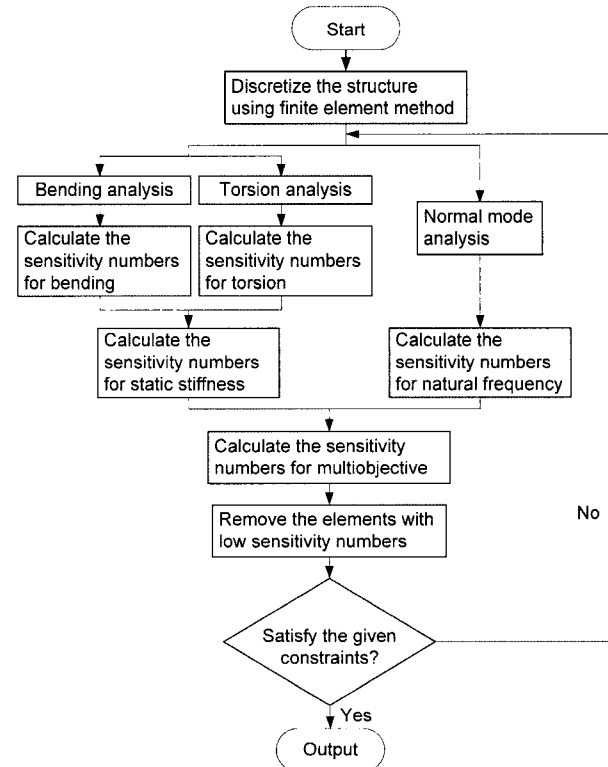


Figure 2. Flowchart for a multi-objective topology optimization.

Equation (10), and the following requirement for the sum of the weighting factors, Equation (11), should be satisfied.

$$\alpha^f = \left(\sum_{i=1}^m w_i V_i \alpha_{Nmi}^f \right) / \left(\sum_{i=1}^m w_i V_i \right) \quad (10)$$

$$\sum_{i=1}^m w_i = 1 \quad (11)$$

Here, α^f is the multi-objective sensitivity number by suppression, w_i represents the filter parameter, V_i denotes the connecting elemental volume, and m is the number of connected elements.

It is clear that the second order scheme may provide a better correction to these numerical instabilities than the first order scheme. In this study, the second order scheme was implemented.

4. APPLICATION EXAMPLES

4.1. Multi-objective Topology Optimization

A flowchart for a multi-objective topology optimization is shown in Figure 2. In order to investigate the effect of curvature of a vehicle's hood on an optimal topology, multi-objective topology optimizations were performed for two cases: (1) a hood with a certain curvature in the y-z plane as shown in Figure 3(c) (Model 1), and (2) a hood with a larger curvature than that of Model 1 in the y-z plane as shown in Figure 3(d) (Model 2). A load of 10 N each was applied at the both ends of the front edge and the center of the hood in order to estimate the static stiffness of bending and torsion, but there was no load to estimate the natural frequency. The center on the front edge and both ends on the back edge were fixed as constraints.

The five weighting factors considered were 0, 0.25, 0.5, 0.75, and 1 in order to reflect the importance of as the static stiffness and natural frequency, respectively. The dimensions and material properties of a vehicle's hood shown in Figure 3(a) are as follows: length (x-axis)=1.122 m, width (z-axis)=1.4 m, Young's modulus=210 GPa, Poisson's ratio=0.3, density=7,800 kg/m³, and thickness=3 mm. The final mass was restricted as 50% of the initial design (original model). The dimensions and the finite element modeling for Model 1 are shown in Figure 3. The overall design region of Model 1 is shown in Figure 3(a) and the finite element modeling in the x-y plane and the y-z plane are shown in Figure 3(b) and Figure 3(c), respectively. The dimensions and the finite element modeling for Model 2 are shown in Figure 3(d). A Pareto-optimal topology solution when the weighting factors for the bending and torsion, λ_1^s and λ_2^s , were 0.5 for Model 1 and Model 2 due to several combinations of

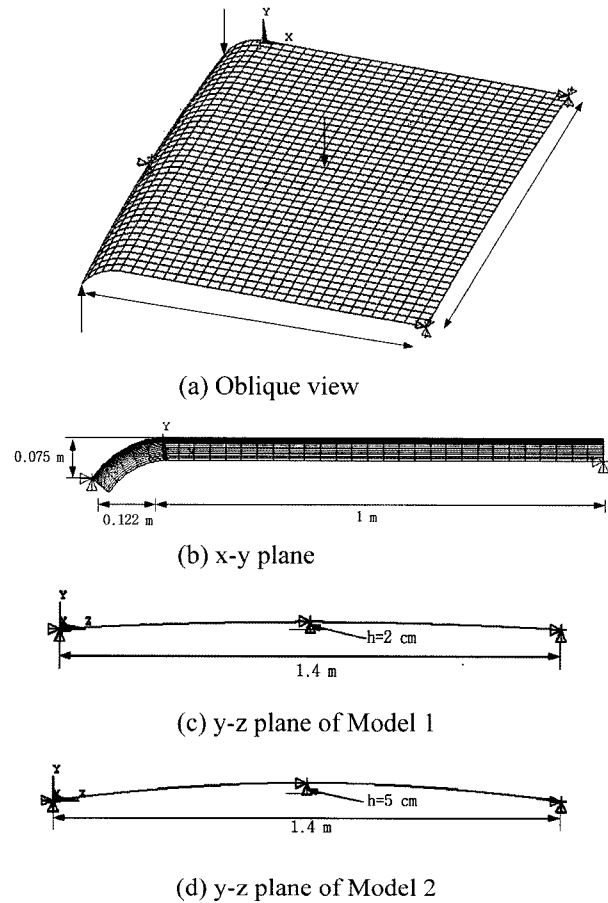


Figure 3. Finite element modeling of vehicle's hood.

weighting factors is shown in Figure 4. It was verified that as the weighting factor for natural frequency, λ_2^m went from 0 to 1 for Model 1 and Model 2, the optimal topologies transmitted from the optimal topology of the static stiffness problem to that of the natural frequency problem. From the Pareto-optimal topology solution shown in Figures 4(a) and 4(b), it is known that the topology of the inner reinforcement of a vehicle's hood used currently is close to that when the weighting factor for the static stiffness, $\lambda_1^m = 1$ or 0.75. The comparison of the first natural frequency and the maximum displacement for Model 1 and Model 2 is shown in Table 1 and Table 2. From the comparison of Table 1, as the weighting factor for the static stiffness, λ_1^m , increased, the maximum displacement decreased for Model 1 and Model 2. Furthermore, from the comparison of Table 2, As the weighting factor for the static stiffness, λ_1^m , increased, the maximum natural frequency decreased for Model 1 and Model 2. From Figure 4(c), 4(d), and 4(e), it was found that the effect of torsion in static stiffness disappeared if the weighting factor for static stiffness, λ_1^m , was smaller than 0.5.

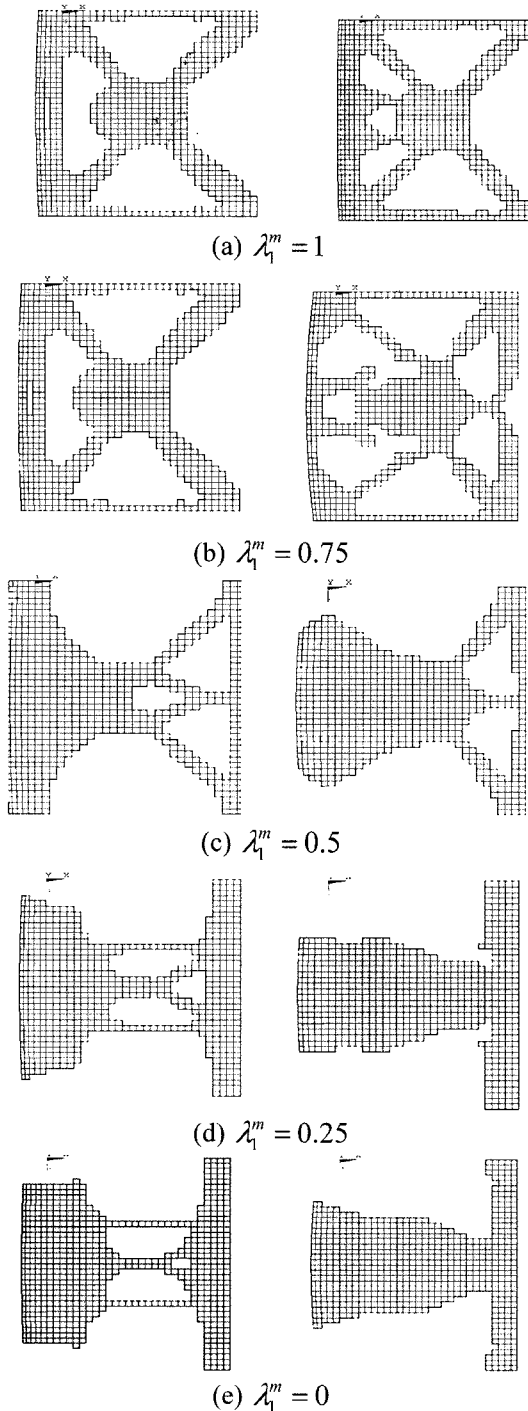


Figure 4. Pareto-optimal topology solution for Model 1 and Model 2.

Therefore, it was verified that the Pareto-optimal topology solution can be reasonably obtained due to the importance of static stiffness and natural frequency. Also, it was shown that Model 2 has a larger static stiffness and

Table 1. Comparison of the maximum displacements (m) for Model 1 and Model 2.

Weighting factor	Model 1	Model 2
$\lambda_1^m = 1$	1.501e-4	1.078e-5
$\lambda_1^m = 0.75$	1.792e-4	6.122e-5
$\lambda_1^m = 0.5$	3.368e-4	1.122e-4
$\lambda_1^m = 0.25$	3.937e-4	1.316e-4
$\lambda_1^m = 0$	–	–

Table 2. Comparison of the natural frequency (Hz) for Model 1 and Model 2.

Weighting factor	Model 1	Model 2
$\lambda_1^m = 1$	9.544	11.108
$\lambda_1^m = 0.75$	9.672	12.353
$\lambda_1^m = 0.5$	11.204	12.875
$\lambda_1^m = 0.25$	13.548	13.816
$\lambda_1^m = 0$	13.668	14.283

more natural frequency than those of Model 1 from Table 1 and 2. From the above result, it was found that a vehicle's hood with the higher curvature is advantageous to achieve the maximum static stiffness and natural frequency.

5. CONCLUSIONS

In this study, based on the ESO method implementing the suppression checkerboard scheme, topology optimization of the inner reinforcement for a vehicle's hood considering static stiffness of bending and torsion as well as natural frequency was performed through multi-objective optimization. A Pareto-optimal topology solution was reasonably obtained due to the importance level of static stiffness and natural frequency. It was also found that models with higher curvature have larger static stiffness and natural frequency than the lower curvature models. Moreover, it was found that hoods of vehicles with the higher curvatures are advantageous for maximum static stiffness and natural frequency. Therefore, it was concluded that the ESO method with a smoothing scheme can be effectively applied to topology optimization of the inner reinforcement of a vehicle's hood.

ACKNOWLEDGEMENT—This work was supported by the Korea Research Foundation Grant funded by Korea Government (MOEHRD, Basic Research Promotion Fund) (KRF-2005-079-BM0036) and the BK21 project of the Korea Research Foundation.

REFERENCES

- Bendsøe, M. P. and Kikuchi, N. (1988). Generating optimal topologies in structural design using a homogenization method. *Comp. Methods Appl. Mech. Eng.*, **71**, 197–224.
- Bureerat, S. and Limtragool, J. (2006). Performance enhancement of evolutionary search for structural topology optimisation. *Finite Elements in Analysis and Design*, **42**, 547–566.
- Chu, D. N., Xie, Y. M., Hira, A. and Steven, G. P. (1996). Evolutionary structural optimization for problems with stiffness constraints. *Finite Elements in Analysis and Design*, **21**, 239–251.
- Lee, T. H., Lee, D. K., Koo, J. K., Han, S. Y. and Lim, J. K. (2000). Optimization of the path of inner reinforcement for an automobile hood using design sensitivity analysis. *Trans. Korean Society of Mechanical Engineers A*, **24**, 62–68.
- Li, Q., Steven, G. P. and Querin, O. M. and Xie, Y. M. (2000). Structure topology design with multiple thermal criteria. *Engineering Computations*, **17**, 715–734.
- Sigmund, O. and Petersson, J. (1998). Numerical instabilities in topology optimization: a survey on precedures dealing with checkerboards, mesh-dependencies and local minima. *Structure Optimization*, **16**, 68.
- Swan, C. C. and Kosaka, I. (1997). Voigt reuss topology optimization for structures with linear elastic material behaviours. *Int. J. Numerical Methods in Engineering*, **40**, 3033–3057.
- Wang, S. M., Moon, H. G. and Ki, S. H. (1999). A synthetic procedure for design of reinforcement. *Spring Conf. Proc.*, **2**, *Korean Society of Automotive Engineers*, 405–410.
- Xie, Y. M., Felicetti, P., Tang, J. W. and Burry, M. C. (2005). From finding for complex structures using evolutionary structural optimization method. *Design Studies*, **26**, 55–72.
- Xie, Y. M. and Steven, G. P. (1994). Optimal design of multiple load case structures using an evolutionary procedure. *Eng. Computations*, **11**, 295–302.